A Monte Carlo Study on the Effect of Various Neutron Capturers on Dose Distribution in Brachytherapy with ^{252}Cf Source

Firoozabadi M. M.[1]*, Izadi Vasafi Gh.[1], karimi-sh K.[1], Ghorbani M.[2]

[1]Department of Physics, Faculty of Sciences, University of Birjand, Birjand, Iran
[2]Biomedical Engineering and Medical Physics Department, Faculty of Medicine, Shahid Beheshti University of Medical Sciences, Tehran, Iran

ABSTRACT

Background: In neutron interaction with matter and reduction of neutron energy due to multiple scatterings to the thermal energy range, increasing the probability of thermal neutron capture by neutron captures makes dose enhancement in the tumors loaded with these materials.

Objective: The purpose of this study is to evaluate dose distribution in the presence of ^{10}B, ^{157}Gd and ^{33}S neutron capturers and to determine the effect of these materials on dose enhancement rate for ^{252}Cf brachytherapy source.

Methods: Neutron-ray flux and energy spectra, neutron and gamma dose rates and dose enhancement factor (DEF) are determined in the absence and presence of ^{10}B, ^{157}Gd and ^{33}S using Monte Carlo simulation.

Results: The difference in the thermal neutron flux rate in the presence of ^{10}B and ^{157}Gd is significant, while the flux changes in the fast and epithermal energy ranges are insensible. The dose enhancement factor has increased with increasing distance from the source and reached its maximum amount equal to 258.3 and 476.1 cGy/h/µg for ^{157}Gd and ^{10}B, respectively at about 8 cm distance from the source center. DEF for ^{33}S is equal to one.

Conclusion: Results show that the magnitude of dose augmentation in tumors containing ^{10}B and ^{157}Gd in brachytherapy with ^{252}Cf source will depend not only on the capture product dose level, but also on the tumor distance from the source. ^{33}S makes dose enhancement under specific conditions that these conditions depend on the neutron energy spectra of source, the ^{33}S concentration in tumor and tumor distance from the source.

Keywords

Brachytherapy, Neutron Capture, ^{252}Cf, Dose, MCNP

Introduction

Californium-252 is an artificial element with a half-life of 2.645 years, and it decays via either alpha emission (96.9%) or spontaneous fission (3.1%). ^{252}Cf emits both photons and neutrons (2.31×106 n/s/µg) of varied energy with potential for both clinical brachytherapy and neutron capture therapy (NCT) applications. The relatively high neutron yield and long half-life, when compared to other spontaneous fissioning isotopes, make ^{252}Cf the best isotope choice for developing a neutron brachytherapy source [1].

Californium-252 has been used as a brachytherapy source since the

*Corresponding author:
M. M. Firoozabadi
Department of Physics, Faculty of Science, University of Birjand, Birjand, South Khorasan, Iran
E-mail: mfiroozabadi@birjand.ac.ir

Received: 20 November 2015
Accepted: 10 February 2016

early 1970s. Clinical successes with ^{252}Cf sources are undoubtedly due in part to the theoretical advantages inherent in treating tumors with fast neutrons in general and with ^{252}Cf in particular [2]. The effectiveness of ^{252}Cf might further be improved by augmenting the ^{252}Cf dose to tumor with an additional dose by neutron capturer loading to the tumor itself. Fast neutrons emitted by the ^{252}Cf source scatter in tumor tissue and lose their energy by multiple scattering to eventually become thermal. Increasing the probability of occurrence thermal neutron capture by neutron capturer cases dose rate enhancement in tumors loaded with these materials [3, 4].

Materials such as ^{10}B, ^{157}Gd and ^{33}S have been proposed as agents for neutron capture. Indeed, the combination of ^{252}Cf brachytherapy and neutron captures may improve tumor dose noticeably. Following the capture by ^{10}B (BNCT), high linear energy transfer (LET) alpha particles and 7Li nuclei are released. These heavy particles deposit their energy in the range of 5-9 mm (tumor cell limit) and therefore, the destructive effects of the resulted particles are limited to boron loaded cells [5, 6, 7]. The method gadolinium neutron capture therapy (GdNCT) is a recently proposed therapy modality, mainly based on the action of Auger and internal conversion electrons generated by ^{157}Gd after neutron capture. The capture reaction in ^{157}Gd has the form of $^{157}Gd\ (n, \gamma)^{158}Gd$ and the emitted gamma rays make dose enhancement [8, 9]. The potential effect of enhancing NCT near the surface of the target volume by addition of ^{33}S has been proposed as well. The neutron capture reaction for ^{33}S has the form of $^{33}S(n, \alpha)^{30}Si$ and has its most important resonance at 13.5 keV. In a study by Porras, an enhancement of the neutron absorbed dose by ^{33}S was observed in a high concentration of ^{33}S (between 1 and 10 mg/g), for a monoenergetic neutron source of 13.5 keV and for tumors at small depths [10, 11].

The purpose of this study is to evaluate the dose distribution in the presence of uniform distribution of neutron capturer materials and to determine the effect of these materials on dose rate enhancement in brachytherapy with ^{252}Cf source. Therefore, careful analysis of different components of the radiation field and a detailed characterization of dose distributions in the absence and presence of neutron capturer materials must be carried out. In this study, neutron-ray flux and energy spectra, neutron and gamma dose rates and dose enhancement factor are determined in the vicinity of a ^{252}Cf source in water phantom with and without same concentration (200 ppm) of ^{10}B, ^{157}Gd and ^{33}S using Monte Carlo MCNP5 code

Materials and Methods

Source Geometry

In the present study, a ^{252}Cf applicator tube (AT) source available from Oak Ridge National Laboratory (ORNL) was modelled. The geometry of ^{252}Cf source is shown in Figure 1. The cylindrical active core is made of californium oxide, Cf_2O_3 with 12 g/cm^3 density. The length and radius of the active cylinder is 1.5 and 0.615 cm, respectively, which is located in a primary capsule of Pt/Ir-10 percentage mass, with inner and outer diameters of 1.35 and 1.75 mm, respectively, and inner and outer lengths of 15.50 and 17.78 mm, respectively. The secondary capsule has inner and outer diameters of 1.80 and 2.80 mm, respectively, and inner and outer lengths of 17.82 and 23.14 mm, respectively. The ends of inner and outer capsules are welded and rounded. Further, the 0.635 mm diameter Bodkin eyelet through the secondary capsule is also included in the source [7].

Monte Carlo Simulation

The Monte Carlo simulation of radiation therapy allows accurate prediction of radiation dose distribution delivered to a patient. In the present work, a complete dosimetric data set for the ^{252}Cf AT source in water, in the ab-

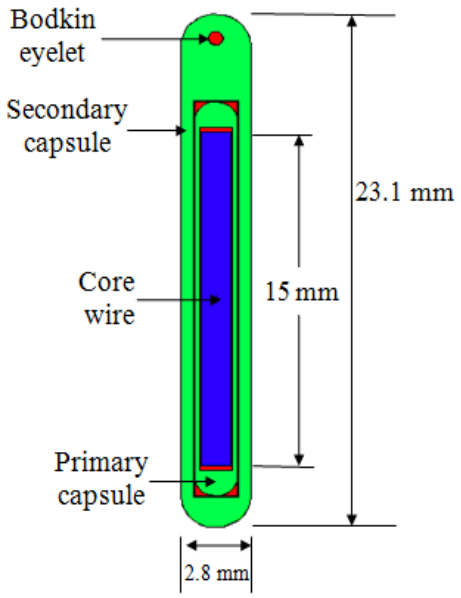

Figure 1: Geometry of ^{252}Cf AT source

sence and presence of neutron capture materials was obtained using Monte Carlo MCNP5 code [12]. The source was positioned in the center of a 15 cm radius spherical phantom filled with water of 0.998 g/cm^3 mass density, or capture materials-water mixture for uniform distribution of ^{10}B, ^{157}Gd and ^{33}S capture materials throughout the water phantom.

The dose rate was determined in a cylindrical annulus 0.2 cm thick×0.2 cm deep positioned along the transverse axis at distances ranging from 0.25 to 10 cm from the source center. Assuming kerma equality with absorbed dose at different distances, F6 tally was used to calculate the particle dose of all components including thermal neutrons, epithermal neutrons, fast neutrons, induced gamma rays and source gamma rays. The neutron dose, source gamma ray and induced gamma ray doses were calculated separately. To calculate particle flux, particle fluence was calculated with F4 tally and then was multiplied by 2.31×10^6, since the calculations were performed assuming one microgram of ^{252}Cf source. The capture product dose (absorbed dose by capture materials) resulted from the capture of thermal neutrons by ^{10}B, ^{157}Gd and ^{33}S was calculated using the fluence-to-kerma conversion factors [13]. The neutron dose is the sum of source fast neutron dose resulted from elastic scattering of fast neutrons in water and the capture product dose which is resulted from thermal neutron capture by ^{10}B, ^{157}Gd and ^{33}S. The neutron energy spectrum for ^{252}Cf source was assumed to be Maxwellian spectrum with an average energy of 2.1 MeV and the most probable energy of ~0.7 MeV [14]. Photon spectrum of the ^{252}Cf source was taken from the study by Fortune, and has photon energies in the range of 0.01–9.79 MeV [15]. The thermal neutron region was defined to be below 0.5eV, the epithermal neutron region is from 0.5eV to 10 keV and the fast neutron region is over 10 keV. The S(α,β) thermal neutron scattering library (lwtr.01t) was used in order to calculate the transport of low energy neutrons. The relative error of calculations was lower than 1%.

Results and Discussion

To validate our Monte Carlo simulation, the computed dose rates were compared with experimental and simulated values published in the literature [16, 17]. Figures 2 and 3 show a comparison between our simulated neutron and total gamma ray dose rates (total gamma ray dose is the sum of source gamma-ray dose and induced gamma ray dose) with the experimental measurements of Colvett [16] and the simulated calculations of Krishnaswamy [17]. There is a good agreement between values with small discrepancies at distances close to the source. These discrepancies might be explained by different modelled energy spectra for neutron and gamma rays emitted from ^{252}Cf source in simulation studies. Also, in the regions close to the source, the dose gradient is extremely steep, and experimental measurement values depend on the accuracy and sensitivity of the measurement device to rapidly changing radiations dose.

After validation, the validated computer code was applied to evaluate the effect of neutron capturers on dose rate distribution. Fig-

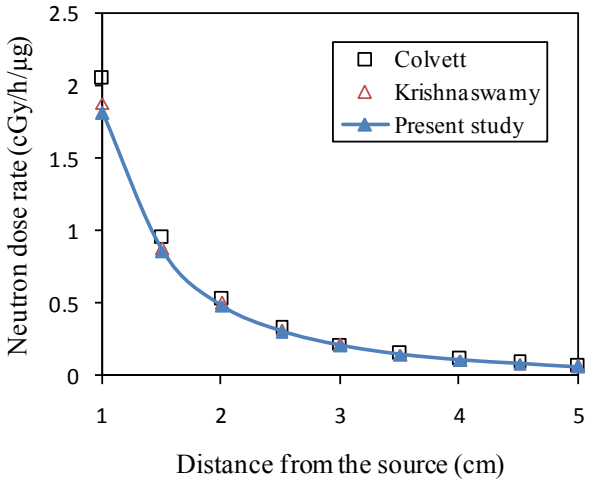

Figure 2: Simulated and experimental neutron dose rates for the water phantom

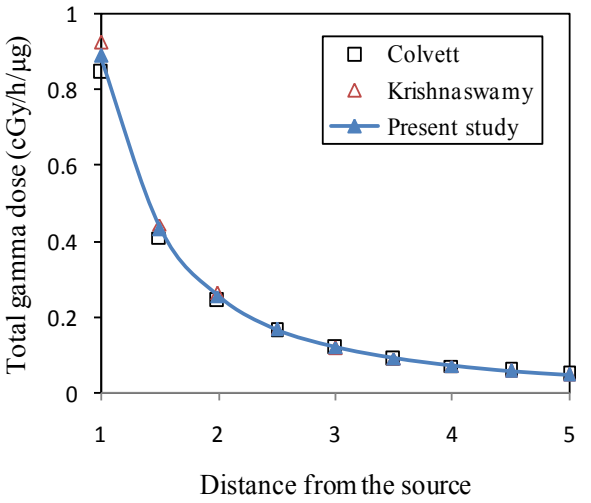

Figure 3: Comparison of total gamma-ray dose rates for the water phantom

ure 4 shows the behavior of the ^{252}Cf neutron energy spectra calculated at the same distance along the transverse direction of the source in water phantom in the absence and presence of capturer materials. As it is seen in this figure, in the presence of ^{157}Gd and ^{10}B capturer materials, neutron flux has decreased in the thermal energy region while it is not seen at the epithermal and fast energy regions. The reduction of thermal neutron flux in the media containing ^{157}Gd and ^{10}B is the direct result of ther-

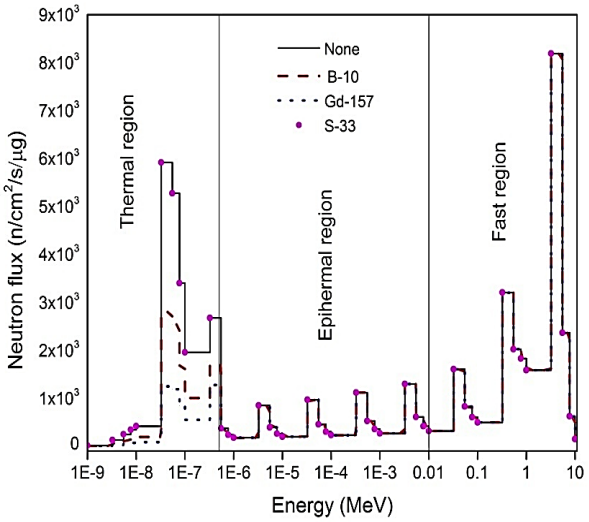

Figure 4: Neutron energy spectrum at 3cm distance from the source, in water phantom with and without the presence of capture materials

mal neutron capture process by these materials and hydrogen in water. Difference in the rate of this reduction depends on the magnitude of thermal neutron capture cross-section of these materials. The no-change in the neutron energy spectrum in the presence of ^{33}S may be resulted from both neutron spectrum of ^{252}Cf source with varied energy and low concentration of ^{33}S in this study.

Figures 5 and 6 show the flux of fast, epithermal and thermal neutrons at different distances from the source in water phantom with and without the presence of capture materials. Obtained result shows that the effect of capture materials on the epithermal and fast neutron fluxes is impalpable. In Figure 6, the thermal neutron flux increases as fast neutrons are scattered mainly by hydrogen and reach a maximum. Afterwards, there is a dramatic decrease due to the absorption of thermal neutrons by capture materials and hydrogen. There is a neutron flux (neutron flux is the sum of thermal, epithermal and fast neutron flaxes) depression of about 57% in ^{10}B, 80% in ^{157}Gd and 0.0005% in ^{33}S loadings. It can be concluded that this depression emanates from the thermal neutron flux depression due to thermal

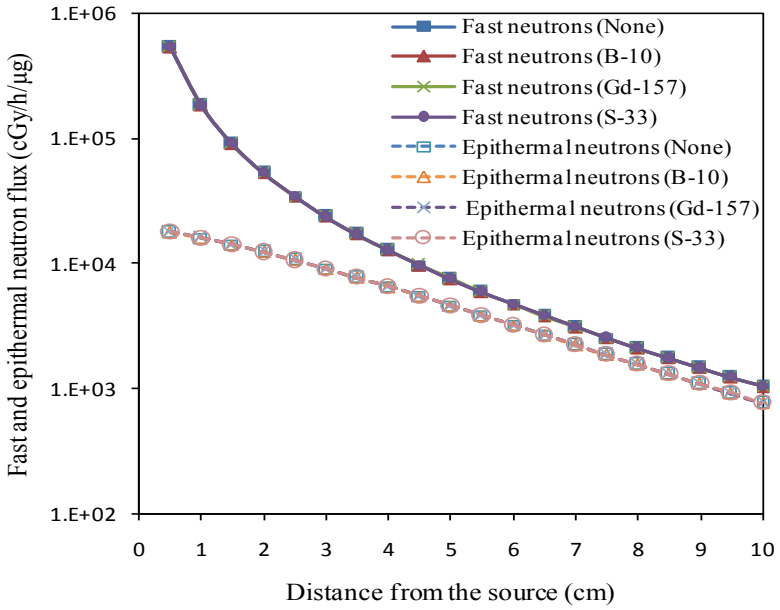

Figure 5: Epithermal and fast neutron fluxes in water phantom in the absence and presence of capture materials

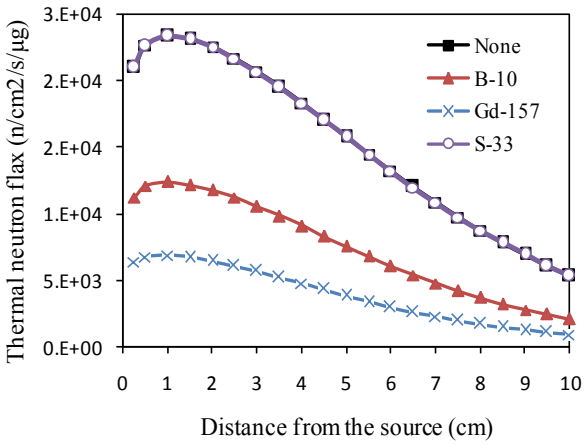

Figure 6: Thermal neutron flux in water phantom in the absence and presence of capture materials

neutron capture by the capture materials.

Figure 7 shows neutron dose rate as a function of distance in water phantom with and without the presence of capture materials. There is significant enhancement of neutron dose in the presence of ^{157}Gd and ^{10}B. It can be concluded that the difference in the amount of this enhancement given that the neutron dose is the sum of source fast neutron ray dose and capture product dose which is resulted from difference in capture product dose rate. In other words, enhancement rate of neutron dose in the presence of capture materials depends on the type of capture products.

Figure 8 provides the comparison between capture product doses in terms of distance from the source. We notice that there is a resemblance and relation between the increase of capture product dose in Figure 8 and depression of thermal neutron flux in Fig 6, with increasing distance from the source. The increase rate of capture product dose resulting from depression of thermal neutron flux is maximum for ^{157}Gd and is minimum for ^{33}S. In other words, the difference in the amount of capture product dose is a direct result of difference in magnitude of the thermalization process of neutrons by these capture materials.

Figure 9 shows the source and the induced gamma ray doses calculated in water phantom with and without the presence of capture materials at different distances from the source. We notice that the existence of capture materials does not alter source gamma dose rate but does reduce the induced gamma dose rate.

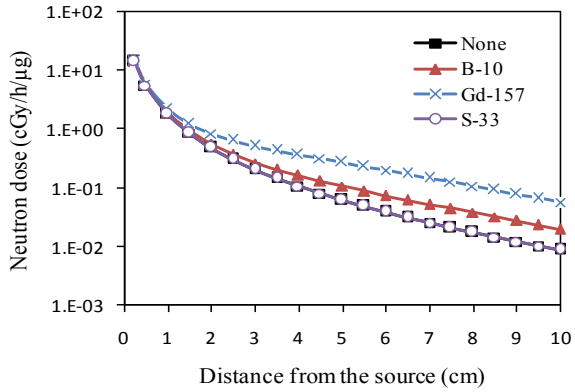

Figure 7: Neutron dose rate distributions in the absence and presence of capture materials at different distances from the source

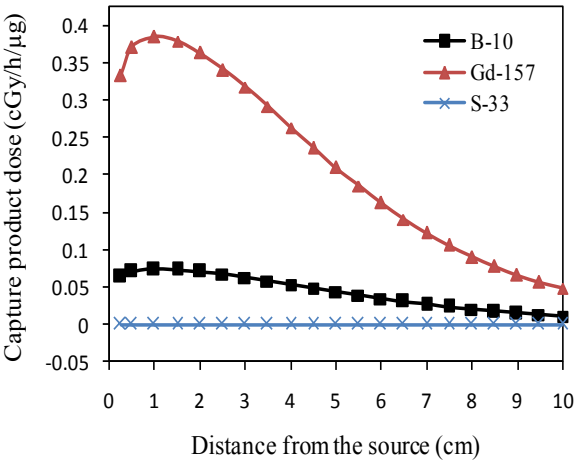

Figure 8: Capture material dose rate distribution for 200-ppm concentrations at different distances from the source

Induced gamma rays are produced by thermal neutron capture reactions of 1H(n,γ)2H in water. The reduction of induced gamma dose in the capture material loading is a result of hydrogen proportion reduction in capture material loaded media compared to only water medium which results in occurrence reduction of thermal neutron capture reactions of 1H(n,γ)2H and, consequently, to reduction of induced gamma dose rate. Contrary to neutron dose, the induced gamma dose in media containing ^{157}Gd is lower than ^{10}B because of higher ability of ^{157}Gd toward ^{10}B in thermal neutron capture which results in fewer thermal neutrons existing to be captured by hydrogen and, induced gamma dose increases in a lower trend in media containing ^{157}Gd. In other words, contribution of induced gamma dose in enhancing total dose rate is further in media containing ^{10}B toward ^{157}Gd.

Figure 10 shows the total dose rate as a function of distance in water phantom in the absence and presence of capturer materials. The enhancement rate of total dose in media containing ^{157}Gd is more than that of ^{10}B and ^{33}S. The reason for it will be due to higher neutron dose and lower induced gamma dose in media containing ^{157}Gd compared to ^{10}B and ^{33}S as higher amount of ^{157}Gd product dose than ^{10}B and ^{33}S.

To determine the effect of capture materials on dose enhancement rate, dose enhancement factor (DEF) is used which is defined as the ratio of total dose in a tumor containing the capture material to total dose in the same tumor without the presence of capture material. Dose enhancement factor values for different capture materials are presented in Table 1. According to data of this table, the value of DEF increases with increasing distance from the source and reaches its highest value equal to 3.258 and 1.476 for ^{157}Gd and ^{10}B, respectively at the distance of roughly 8 cm from the source center, and after that decreases. In other words, the effectiveness rate of ^{157}Gd and ^{10}B capture materials in enhancing dose rate depends on the tumor distance from the source. Increase in the value of DEF with increasing distance from the source despite the decline in ray intensity is due to both decrease neutron average energy in the effect of attenuation, and increasing the less energetic scattered rays arrived to depth that makes increase the occurrence probability of thermal neutron capture by capture materials and subsequently dose rate enhancement. Enhancement rate of total dose in the presence of ^{33}S is not significant since its DEF is equivalent to one.

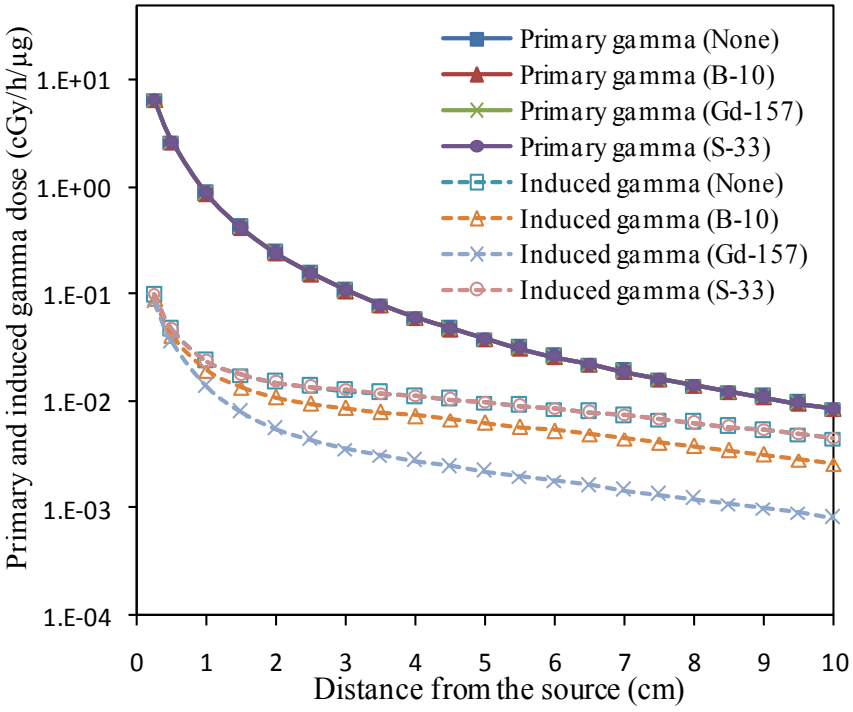

Figure 9: Source and induced gamma ray dose as a function of distance

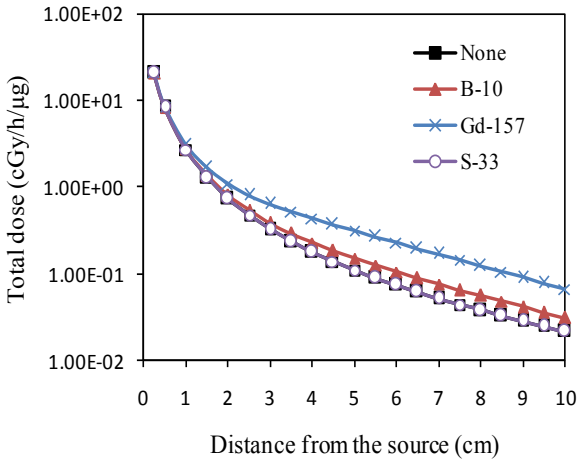

Figure 10: Total dose rate versus distance away from the source

Table 1: Dose enhancement factor at different distance from the source for ^{10}B, ^{157}Gd, and ^{33}S

r (cm)	^{10}B	^{157}Gd	^{33}S
0.5	1.008	1.043	0.999
1	1.026	1.138	0.999
2	1.093	1.478	0.999
3	1.187	1.947	0.999
4	1.286	2.430	1
5	1.373	2.841	1
6	1.437	3.118	0.999
7	1.470	3.255	0.998
8	1.476	3.258	0.998
9	1.461	3.185	1
10	1.428	3.039	0.999

Conclusion

In this study, a detailed characterization of dose distribution in the absence and presence of ^{10}B, ^{157}Gd and ^{33}S neutron capturers has been carried out for ^{252}Cf brachytherapy source using Monte Carlo simulation. Obtained result shows that tumor loading with ^{157}Gd and ^{10}B neutron capturers in neutron brachytherapy with ^{252}Cf source makes significant dose enhancement due to the increase in occurrence probability of thermal neutron capture by these materials. The results also show that the magnitude of dose augmentation with this

therapy design will depend not only on the capture product dose, but also on the tumor distance from the source. This dependence is resulted from both difference in the magnitude of thermalization process of neutrons by these materials and the decrease of neutron average energy due to attenuation that make increase the occurrence probability of thermal neutron capture. ^{33}S is not a suitable agent for dose increase by neutron capture in brachytherapy with ^{252}Cf source. In other words, ^{33}S makes dose enhancement under specific conditions in which these conditions depend on neutron energy spectra of source, the ^{33}S concentration in tumor and tumor distance from the source.

Acknowledgment

The authors are grateful to Birjand University for the financial support of this work.

Conflict of Interest

There is not any relationship that might lead to a conflict of interest. Birjand University has financially supported the work and this is stated in the acknowledgment section of the article.

References

1. Maruyama Y. Californium-252: New radioisotope for human cancer therapy. Endocuriether. *Hyperthermia Oncol*. 1986;**2**:171-87
2. Schlea CS, Stoddard DH. Californium isotopes proposed for intracavity and interstitial radiation therapy with neutrons. *Nature*. 1965;**206**:1058-9. doi.org/10.1038/2061058a0. PubMed PMID: 5839071.
3. Rorer D, Wambersie G. Current Status of neutron capture therapy. *IAEA*. 2001;(8):75-7.
4. Al-Saihati I, Naqvi A. Neutron and gamma ray doses from a 252Cf brachytherapy source in a water phantom. *Journal of Radioanalytical and Nuclear Chemistry*. 2013;**296**:963-6. doi.org/10.1007/s10967-012-2172-5.
5. Ghassoun J, Merzouki A, El Morabiti A, Jehouani A. On the 252 Cf primary and secondary gamma rays and epithermal neutron flux for BNCT. Nuclear Instruments and Methods in Physics Research Section B: Beam Interactions with Materials and Atoms. 2007;263:231-3. doi.org/10.1016/j.nimb.2007.04.091.
6. Yanch JC, Zamenhof RG. Dosimetry of 252Cf sources for neutron radiotherapy with and without augmentation by boron neutron capture therapy. *Radiat Res*. 1992;**131**:249-56. doi.org/10.2307/3578413. PubMed PMID: 1438684.
7. Ghassoun J, Mostacci D, Molinari V, Jehouani A. Detailed dose distribution prediction of Cf-252 brachytherapy source with boron loading dose enhancement. *Appl Radiat Isot*. 2010;**68**:265-70. doi.org/10.1016/j.apradiso.2009.10.004. PubMed PMID: 19889549.
8. Wierzbicki JG, Maruyama Y, Porter AT. Measurement of augmentation of 252Cf implant by 10B and 157Gd neutron capture. *Med Phys*. 1994;**21**:787-90. doi.org/10.1118/1.597324. PubMed PMID: 7935215.
9. Brugger RM, Shih JA. Evaluation of gadolinium-157 as a neutron capture therapy agent. *Strahlenther Onkol*. 1989;**165**:153-6. PubMed PMID: 2494719.
10. Porras I. Enhancement of neutron radiation dose by the addition of sulphur-33 atoms. *Phys Med Biol*. 2008;**53**:L1-9. doi.org/10.1088/0031-9155/53/7/L01. PubMed PMID: 18356577.
11. Porras I. Sulfur-33 nanoparticles: a Monte Carlo study of their potential as neutron capturers for enhancing boron neutron capture therapy of cancer. *Appl Radiat Isot*. 2011;**69**:1838-41. doi.org/10.1016/j.apradiso.2011.04.002. PubMed PMID: 21497099.
12. X-5 Monte Carlo Team, 2005. MCNP-A General Monte Carlo N-Particle Transport Code. Version5. Los Alamos National Laboratory Report LAUR-03-1987. (April 2003; Revised October3.2005)
13. Chadwick MB, Barschall HH, Caswell RS, DeLuca PM, Hale GM, Jones DT, et al. A consistent set of neutron kerma coefficients from thermal to 150 MeV for biologically important materials. *Med Phys*. 1999;**26**:974-91. doi.org/10.1118/1.598601. PubMed PMID: 10436900.
14. Martin R, Miller J, editors. Applications of Californium-252 Neutron Sources in Medicine, Research, and Industry. Americas Nuclear Energy Symposium (ANES 2002); 2002.
15. Fortune IV EC. Gamma and neutron dose profiles near a Cf-252 brachytherapy source. 2010.
16. Colvett RD, Rossi HH, Krishnaswamy V. Dose distributions around a californium-252 needle. *Phys Med Biol*. 1972;**17**:356-64. doi.org/10.1088/0031-9155/17/3/302. PubMed PMID: 5070446.
17. Krishnaswamy V. Calculated depth dose tablets for californium-252 sources in tissue. *Phys Med Biol*. 1972;**17**(1):56-63. doi.org/10.1088/0031-9155/17/1/006. PubMed PMID: 5071502.